$K\alpha$ emission measurements and superthermal electron transport in layered laser-irradiated disk targets

B. Luther-Davies, A. Perry, and K. A. Nugent*
Department of Engineering Physics, The Research School of Physical Sciences, The Australian National University, P.O. Box 4, Canberra, Australian Capital Territory, Australia 2601
(Received 12 November 1986)

We report results from an experimental study of superthermal electron energy transport in planar layered disk targets irradiated at high intensities ($I > 3\times 10^{14}$ W/cm^2) by short (<100-psec) pulses of Nd-laser radiation. The $K\alpha$ emission from a Ni fluor covered by an Al electron-transport layer has been recorded both spatially integrated and spatially resolved over the target surface. By analyzing the results, with the aid of a Monte Carlo electron-transport code, it has been found that electron transport within the target is dominated by a non-Maxwellian group of very energetic electrons ($E_e \approx 50$—200 keV) which carry about 3% of the absorbed laser energy deep within the targets. The spatial distribution of the electrons over the target surface underlines the effect of the coronal magnetic and electric fields on lateral energy transport by superthermal electrons.

I. INTRODUCTION

A wide range of experimental data has been collected on lateral and axial energy transport in laser-irradiated targets. Particularly important in experiments performed using long-wavelength lasers ($\lambda > 1$ μm) at high intensities ($I\lambda^2 > 10^{14}$ W cm^{-2} μm^2) is lateral energy transport by superthermal electrons, which has been shown to be strongly influenced by coronal electric and magnetic fields. Previous experimental results in this regime have shown that a significant fraction (around 30%) of the laser energy absorbed by the plasma is transferred to the superthermal electrons which penetrate the high-density regions of the target. A large fraction of the superthermal electron energy (typically 50%) is deposited in regions of the target outside the focal spot.

The importance of self-generated magnetic fields in this lateral transport process has been demonstrated in computer simulations of short pulse CO_2-laser radiation incident on planar targets.[1] In those simulations the superthermal electrons were driven laterally through the corona by crossed electric and magnetic fields; the former arising from charge separation in the expanding plasma sheath, and the latter from the $\nabla N_h \times \nabla T_h$ thermoelectric source term originating from the superthermal electrons themselves. The dynamics of this process leads to deposition of superthermal electron energy in an expanding ring around the focal spot as has been reported experimentally[2,3] and also observed in the most recent simulations.[4]

In spite of recent developments, the computer models are still too approximate to allow total confidence in their description of the transport processes. Unfortunately, there have been few experimental studies of plasmas in conditions similar to those studied using the codes with which to compare them. In previous work, however, we described measurements of the evolution and spatial structure of self-generated magnetic fields in plasmas created by irradiating planar targets with picosecond duration pulses of Nd-laser radiation.[5] This work provided evidence for the first time that megagauss self-generated magnetic fields grew and decayed during the laser pulse itself and were, hence, most probably generated by the superthermal source term. Furthermore, high resolution hard x-ray images were recorded which qualitatively demonstrated remote energy deposition by the superthermals at the edge of the magnetized region by showing a 300-μm-diameter "ring" of hard—x-ray emission surrounding the focal spot. Both of these features had been observed in the simulations.[1,4]

In this paper we present additional results, recorded in the same experimental conditions as before, of a quantitative study of superthermal energy deposition in the target. By using both time- and space-integrated $K\alpha$ emission measurements from layered targets as well as high-resolution (>15 μm) $K\alpha$ imaging, we have been able to map superthermal electron energy deposition over the target surface with high accuracy. The dependence of the $K\alpha$ signal on the thickness of an Al transport layer covering the $K\alpha$ emitter has been determined for a wide range of laser intensities and shows features that indicate that the superthermal electron distribution is non-Maxwellian.

The experimental details were as follows. The targets consisted of Ni discs 1 mm in diameter and 6.35 μm thick overcoated with an aluminum electron-transport layer of variable thickness. The nickel acted as a fluor emitting $K\alpha$ radiation when penetrated by the superthermal electrons. The choice of the atomic number of the fluor has been discussed by Hares *et al.*[6] and was made, firstly, to be high enough to ensure that the fluor K edge was well above the plasma thermal temperature, to avoid K-shell ionization by the thermal plasma [in this case the thermal temperature has been determined from x-ray measurements to be approximately equal to 500 eV (Ref. 7) which is well below the Ni K edge at 8.332 keV]; and, secondly, to be low enough to prevent K-shell ionization by Bremsstrahlung generated in fluor itself. The minimum thickness of the Al was 1 μm which was much thicker than the known burn depth (determined in previous experiments[8])

of the laser at the maximum intensity used in these experiments. The maximum Al transport layer thickness was 110 μm.

The time- and space-integrated $K\alpha$ emission generated in the fluor was measured using *p-i-n* diode detectors fitted with a nickel/iron Ross-filter pair. In addition, a two-channel penumbral imaging camera[9] fitted with identical filters was used to spatially resolve the $K\alpha$ emission patterns from the fluor with a best resolution of about 15 μm although in some of the results presented later the resolution was reduced to about 50 μm to improve the signal-to-noise ratio in the reconstructed images. Both the x-ray diodes and the penumbral imaging camera viewed the targets from the rear (i.e., from the Ni side) at 45° to the axis of the laser beam. The x-ray images were recorded on Agfa X-OMAT film.

The targets were irradiated at normal incidence using 0.6—2-J pulses of either 20- or 100-psec duration at 1.054 μm from a single beam Nd:glass laser. The beam was focused onto the targets using $F=1$ optics and the target position adjusted relative to best focus to vary the laser intensity. The intensities used range from 2.5×10^{14} to greater than 3×10^{17} W/cm^2. The filtered x-ray diodes measured the $K\alpha$ signal as a function of aluminum overlayer thickness and laser intensity, while the images gave additional information by determining the spatial distribution of the $K\alpha$ signal.

The time- and space-integrated $K\alpha$ signals as a function of Al overlay thickness for different laser intensities (20-psec duration pulses) are shown in Fig. 1. In obtaining these data a number of interesting features were observed. It was found, for example, that the $K\alpha$ yield was independent of laser energy in the range 0.6—2.0 J. Previous measurements of the total absorption by the target obtained using a box calorimeter[8] had demonstrated that the absorbed fraction did not, however, vary. This, therefore, implied that the number of superthermals penetrating the target was fixed, perhaps by some time-dependent transport inhibition mechanism. This idea is consistent with results on time-resolved $K\alpha$ emission from CO_2-laser experiments[10] where the duration of the $K\alpha$ signal recorded using an x-ray streak camera was found to be much shorter than the laser-pulse duration. Those results indicated that either a transport inhibiting process switched on, or superthermal electron generation switched off, early in the pulse. We searched for similar behavior in these experiments by stretching the laser pulse to about 400 psec and monitoring the $K\alpha$ signal collected by a pentaerythritol (PET) Von Hamos crystal spectrometer with a Hadland X-CHRON streak camera. Low signal levels prevented good data from being obtained, but in some instances $K\alpha$ signals of much shorter duration than the laser pulse were recorded, although this behavior was far from repeatable. It is worth noting that a relative insensitivity of the $K\alpha$ signal-to-laser energy has been reported previously by Mitchell *et al.*[11] They explained their observation by suggesting that an increase in the laser energy was accompanied by an increase in the hot-electron temperature which then caused the $K\alpha$ signal to originate from deeper within the target. As a result, self-absorption of the $K\alpha$ signal as it emerged in the direction of the detector increased helping to "clamp" the $K\alpha$ signal level. This explanation cannot be applied in our case because we used a thin fluor viewed from the rear rather than a thick fluor viewed from the front as was the case in Mitchell *et al.*'s work.

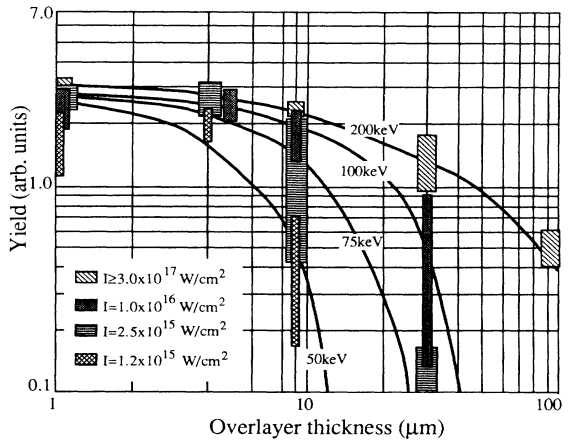

FIG. 1. Spatially integrated $K\alpha$ emission data as a function of overlayer thickness and laser intensity. The solid curves are yield predictions calculated using the Monte Carlo code and a monoenergetic, spatially beamlike electron distribution.

Figure 1 shows that the $K\alpha$ signal varies little when the Al overlayer thickness is less than about 5 μm. The signal, however, decreases when the Al thicknesses increases from 5 to 100 μm at a rate depending on the laser intensity, with the behavior qualitatively suggesting that the highest laser intensities produce the most penetrating electrons, as would be expected. The shape of these curves, however, differs significantly from the predictions based on electron-transport models such as those used by Harrach and Kidder[12] which show (for a Maxwellian electron distribution with a temperature in the range 10—50 keV) a more rapid variation than is observed here in the signal for Al thicknesses between 1 and 10 μm. Our curves are particularly flat below about 5 μm at all intensities, but drop off rapidly above 5 μm, especially at low laser intensities.

We examined the possibility that with the thinnest Al overlays the hot electrons were orbiting the target rather than penetrating through the transport layer to the rear. This was ruled out due both to the fact that the large diameter of the targets relative to their thickness would then make it unlikely that a small change in target thickness, from 10 to 20 μm, say, would have any effect on this process at all, and yet a distinct drop in the $K\alpha$ signal was observed; and also because the x-ray images showed that most of the $K\alpha$ emission was confined to a region less than 800 μm in diameter surrounding the focal spot and did not extend to the target edges. It seemed clear, therefore, that the signal had to be caused by electrons passing through the Al transport layer.

There are at least three possible explanations for the shape of our curves. Firstly, models such as Harrach and Kidder's, which are based upon Spencer's[13] semiempirical model of electron transport, could incorrectly predict energy deposition in thin, layered foils. Secondly, the hot-

electron distribution could be non-Maxwellian, and thirdly, there could be processes which affect electron transport in the solid which are not included in any of the models.

The reason for doubting the accuracy of the energy transport model are as follows. Spencer's model is only applicable, strictly speaking, to an electron source embedded within an infinite, homogeneous material. Energy deposition profiles are then calculated assuming the source is of a particular type, i.e., beamlike, point isotropic or plane isotropic. Errors can result when this model is applied to finite, multilayer targets for two reasons. Firstly, since Spencer's model assumes that the target is infinite, energy deposition near the source is influenced significantly by electrons returned by backscattering from deep within the target. This is quite important for moderate Z materials where the albedoes (the fraction of the incident energy that is backscattered) are significant, especially for isotropic or semi-isotropic sources. In finite targets the albedoes will, obviously, be different because of the limited depth of the material, and this introduces an error when calculating the energy deposited in the transport layer.

In addition, the boundaries between the different atomic number materials in a layered target will backscatter electrons. As a result some method must be used with Spencer's model to describe backscattering from one layer to the next and, specifically, to calculate how much ionization the electrons cause before they are backscattered out of the fluor. This is normally done by incorporating experimentally determined backscatter data into the Spencer model.[6] These data commonly consist of measurements of the fraction of electrons of all energies backscattered from a metal target and the albedoes. However, the K-shell ionization that is produced can only be calculated when the *energy spectrum* of the backscattered electrons is known. That information is not normally available, and in any case it is difficult to incorporate into the model. Furthermore, the experimental data are usually obtained using semi-infinite targets, and as pointed out above, the amount of backscatter will in any case be different for a thin target.

It could be argued that backscattering is unimportant because the plasma recycles the electrons and so even if the albedo is large, this "lost" energy will be returned to the target. The problem with this argument is that although the incorrect backscatter analysis may give a reasonable result for the *total energy* deposited within a multilayer target, it will give incorrect results for the energy deposited *in each individual layer*. Since the latter quantity is what is needed to characterize the $K\alpha$ yield, the errors introduced by incorrect modeling of the backscatter can be significant. To reduce these errors, we, therefore, used an improved model to describe electron energy transport. This model has also been used to investigate other phenomena, such as the effect of different electron distributions on the $K\alpha$ yield.

II. A MONTE CARLO ELECTRON-TRANSPORT MODEL

In order to more accurately model energy transport and deposition in multilayer target, a Monte Carlo electron transport code has been developed based on that described by Salvat and Parellada[14] but adapted to predict $K\alpha$ yields. This code describes both elastic and inelastic scattering by using model cross sections for both processes. Knowing the cross sections, the electron trajectories are calculated in the following way. An electron with some initial energy E_0 starts at the surface of the target. The cross sections are calculated for both the elastic and inelastic scattering and summed to give the total cross-section σ_t from which the electron mean free path is calculated. The probability density for the next step having a length s is given by

$$P(s)=N\sigma_t\exp(-sN\sigma_t)\ , \tag{1}$$

and the step length is sampled from this distribution. The type of collision that occurs at the end of the step is randomly chosen to fit a probability density defined by the relative cross sections of the two scattering processes. If the collision is elastic, the momentum transfer for the collision is sampled from the probability density (P) function

$$P(q)=\frac{1}{\sigma_\pi}\frac{\partial\sigma_e}{\partial q}\ , \tag{2}$$

where σ_π is the cross section for scattering through π. The scattering angle is then obtained from the relationship between angle and momentum transfer (q).

If the collision is inelastic, the minimum energy loss is calculated, $W_{\min}$, and the energy loss chosen from an inverse parabolic distribution lying between $W_{\min}$ and E_e (the electron energy). The scattering angle in this inelastic collision is calculated using a binary collision model.

At each inelastic collision the direction of motion is reset and the cross sections, step length, etc., are recalculated and the process repeated. For an elastic collision, the mean free path remains the same with only the direction of motion changed. This procedure is followed until the electron energy falls below the K-edge energy of the fluor or the electron leaves the target. In the latter case the electrons can optionally be recycled, i.e., they can be allowed to reenter the target from the rear. The angular, spatial, and energy distributions of the backscattered and transmitted electrons can be recorded for comparison with experimental data to check the performance of the code. The scattering cross sections include relativistic corrections and, hence, can be expected to be accurate for electron energies up to several hundred keV. This is important because the high-energy tail of the Maxwellian distribution will produce significant fluorescence even with relatively low-electron temperatures.

The calculation of the $K\alpha$ yields using such a code could be performed in a number of ways. To reduce computational time we adopted a simplified approach used also in the Spencer model, namely, we assumed that on average a specific (energy dependent) fraction of the electron energy lost during each collision appears as $K\alpha$ emission. The fluorescence yield was included in the calculation of that fraction. Such a procedure averaged over tens of thousands of collisions will give a good estimate of the total $K\alpha$ yield. The remaining problem is then to determine the energy dependence of the $K\alpha$ cross section. A

number of empirical estimates are available[15,16] as well as theoretical models including, in some cases, relativistic corrections.[17] A compilation of available predictions and experimental data show considerable discrepancies (25—50%) between these different results. We chose to use the empirical fit suggested by Drawin[16] which, for example, provides quite good agreement with recent experimental data from Jessenberger and Hink[18] but predicts values considerably greater than earlier formulations.[15]

The code was tested by modeling experimental data on the transmission and backscatter of electron beams through thin foil targets and provided results which were excellent fits to the measurements. We then used it to test one specific assumption often used in the calculation of energy deposition profiles in targets, namely, that it is safe to assume that the angular distribution of the electrons entering the target is isotropic. This is often justified by assuming that the plasma itself produces an isotropic distribution, although experimental data suggests that this is only a good assumption at high laser intensities and when the distribution is spatially averaged over the target surface.[19] Alternatively, it has been asserted that scattering within the first few microns of the transport layer does, in any event, isotropize the angular distribution.[12] Although such an assumption may be valid for rather low-energy electrons, plenty of experimental data on electron beam transport through metal films exists to refute it, especially for energies above about 20 keV.[20] Since these are just the energies producing fluorescence in our experiments, then the change in $K\alpha$ yield with the angular distribution of the electrons is worth investigating, especially when space-resolved data are available.

Figures 2(a) and 2(b) show the variation of $K\alpha$ yield as a function of electron temperature for a Maxwellian electron distribution for the two cases when the source was point isotropic or beamlike. In these calculations a significant fraction of the electron energy was transmitted through the foil in a single pass and in generating Fig. 2 all these transmitted electrons were recycled, i.e., they were made to reenter the target from the rear. Increased electron penetration in the case of the beamlike source is apparent because it creates slightly more (by about 10—20%) $K\alpha$ emission than the isotropic distribution at the same temperature when the overlay thickness is less than about 20 μm; however, the yield drops more rapidly for overlayer thickness above 20 μm. Curves for the beamlike source are, therefore, closer to the experimental data than those for the isotropic source.

The Monte Carlo code allows the individual trajectories of the electrons to be mapped through the target. As a result it is easy to demonstrate that the low-energy electrons are rapidly isotropized as they penetrate the transport layer causing them to lose a large fraction of their energy. On the other hand, the high-energy electrons pass essentially undeviated through to the fluor.

This suggests that if the low-energy electrons were not present, then the shape of the $K\alpha$ yield curves would become closer to the experimental data. An extreme case would be to replace the Maxwellian distribution with a monoenergetic source. Results for this case assuming the source is spatially beamlike, with the transmitted electrons

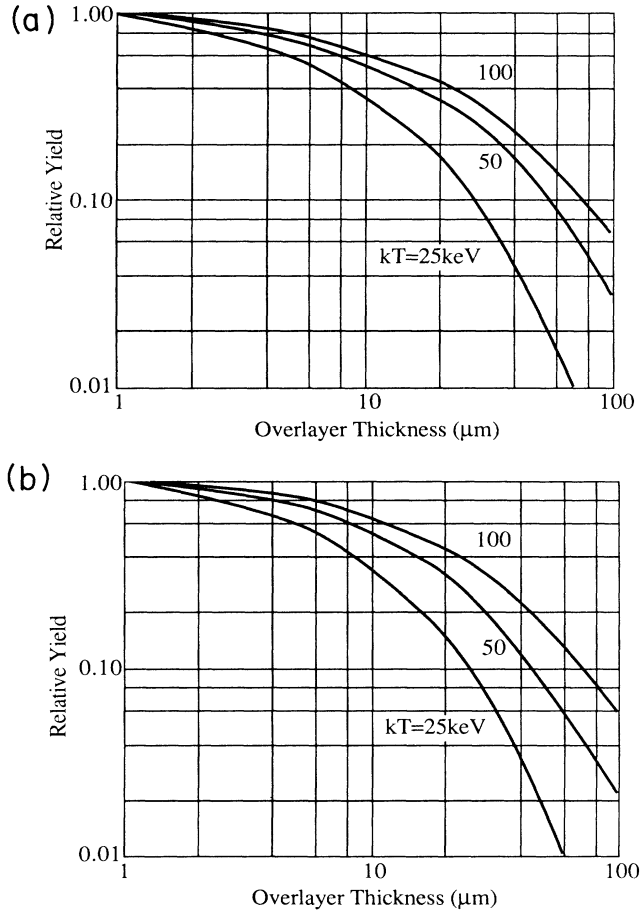

FIG. 2. (a) Predicted $K\alpha$ yield as a function of temperature for a Maxwellian electron distribution and point isotropic source distribution. (b) As (a) but assuming a spatially beamlike distribution with one degree of freedom.

recycled, are shown for comparison with the experimental data in Fig. 1. Examination of these curves shows that they are quite flat in the 1—9-μm region and also drop rapidly above 9 μm because of the absence of fluorescence generating electrons in the high-energy tail of the distribution. As a result, curves for the beamlike, monoenergetic source fit the experimental results quite well with a beam energy of $\approx$50 keV at 10^{15} W/cm^2, $\approx$100 keV at 10^{16} W/cm^2, and $\approx$200 keV at $\approx 3\times 10^{17}$ W/cm^2 (the solid lines in Fig. 1). This result suggests that the superthermal distribution entering the target is probably deficient in both low- and high-energy electrons.

A further point warrants examination, namely, the fact that we have recycled all the electrons transmitted through the target. This might be wrong and could affect the shape of the yield curves. A comparison of curves for a beamlike Maxwellian source as well as those for a monoenergetic source with and without recycled electrons demonstrated, however, that the differences in the shape of the curves are generally small. Experimentally we searched for evidence that the transmitted electrons left the back of the target to strike the chamber walls, etc., by

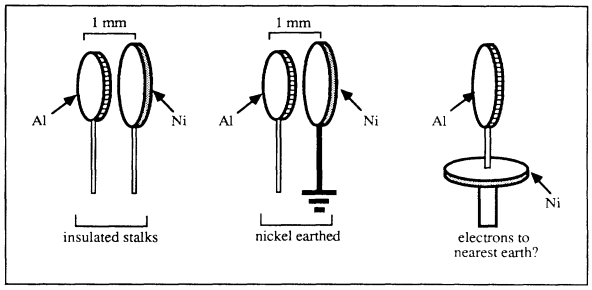

FIG. 3. Target geometries used to search for evidence that transmitted electrons left the target.

comparing the x-ray emission from a series of double targets shown in Fig. 3. Any electrons crossing the vacuum gap between the laser-irradiated disc and the subsidiary Ni fluor should be detectable by the presence of a $K\alpha$ signal from the Ni. In none of the geometries used was this observed. It is possible that some of the energy of the transmitted electrons is dissipated in fast ion acceleration on the rear side of the foil. This has been observed experimentally,[21] and suggests that modeling the distribution of electron energies return to the rear surface can be quite complex especially if the transmitted electron beam generates a magnetic field on the rear of the target.[22] Fortunately, the shape of the yield curves does not vary much whether the transmitted electrons are recycled or not, although the absolute yield does change by a large factor (3—5).

The time- and space-integrated $K\alpha$ signals were used to estimate the fraction of the absorbed energy transported into the target by the superthermal electrons. Using the known sensitivity of the p-i-n diode x-ray detectors and the $K\alpha$ conversion efficiencies determined by the code, assuming that all transmitted electrons were recycled, we found that this corresponded to approximately 3% of the absorbed laser energy or about 1% of the incident laser energy. These values are much below those quoted in previous work. However, the use of a model based on the Spencer approach to electron transport will provide a very different estimate of the conversion efficiency from electron energy to $K\alpha$ x-ray emission in comparison with the Monte Carlo code, basically because transmitted electrons are always assumed lost when using the Spencer approach. Because of this our estimate would increase if we used the Spencer formulation to indicate about 15% of the absorbed energy was entering the target in the form of hot electrons, bringing our result closer to previous values. In our particular experiments, however, we have supporting evidence that the total energy deposited by the hot electrons cannot exceed 10% of the absorbed energy and, hence, our results differ significantly from the values as high as 57% reported earlier.[3,6,23] The supporting evidence consisted of measurements of absorption and energy partition in the same laser conditions and was obtained using ion and scattered light calorimetry.[8] This showed that more than 90% of the absorbed energy was transferred to moderate to high-energy ions ruling out the possibility that energy deposition by the hot electrons had

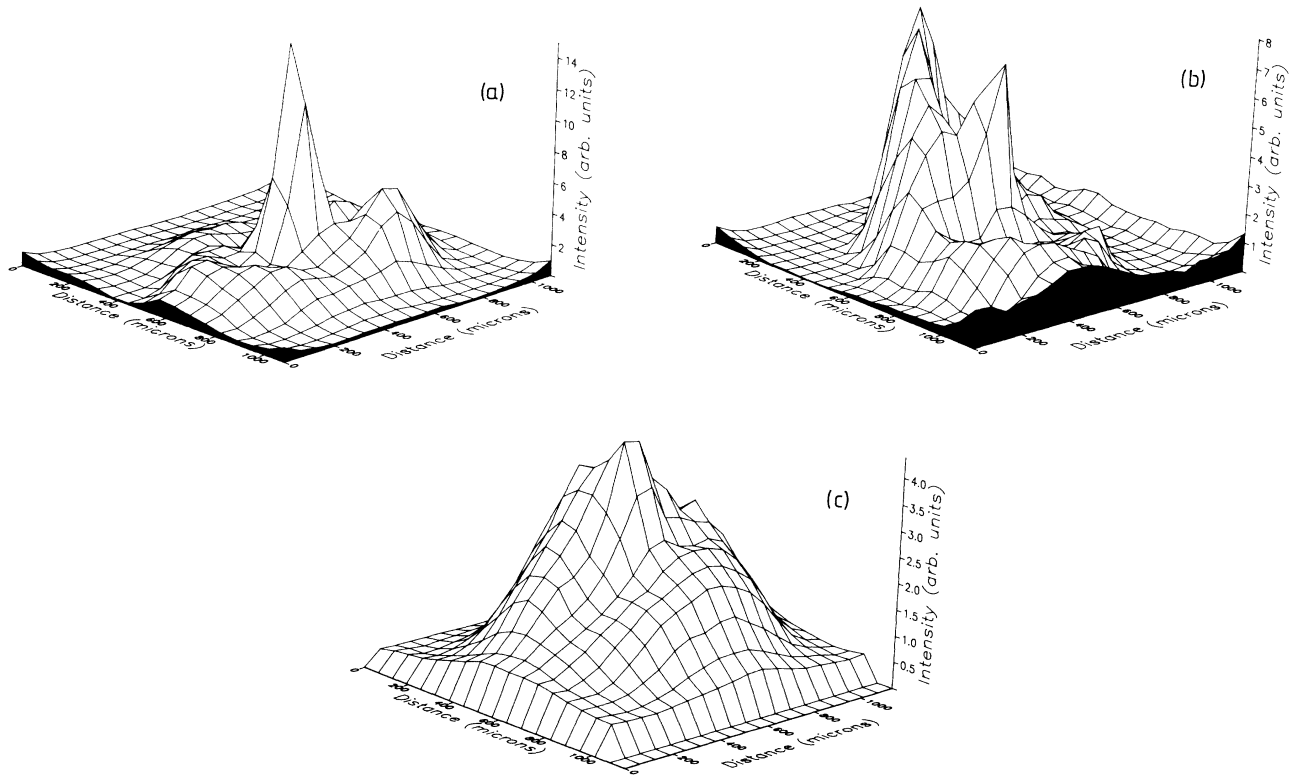

FIG. 4. Spatially resolved $K\alpha$ emission as a function of overlayer thickness; (a) overlayer 1 μm thick, (b) overlayer 9 μm thick, and (c) overlayer 30 μm thick.

been seriously underestimated. This relatively low-energy density deposited in the fluor by the hot electrons allows us to assume that preheating and ionization were not affecting the $K\alpha$ emission—a necessary assumption for our calculations to be valid.

III. SPACE-RESOLVED $K\alpha$ DATA

A large number of $K\alpha$ images were recorded using the two-channel penumbral imaging camera. These images were characterized by a small region of intense emission from beneath the focal spot surrounded by a broader region of lower intensity emission extending up to about 800 μm in diameter. The relative intensity of the emission from beneath the focus to the remote emission varied depending on the thickness of the Al transport layer. In addition, the emission from outside the focal spot was often quite asymmetrical.

A set of images obtained for a 1-, 9-, and 30-μm overlay thickness are shown in Figs. 4(a)—4(c), respectively. The laser intensity was $\geq 3\times 10^{17}$ W/cm^2 and hence the focal spot was smaller than the camera resolution which was set at ≈ 50 μm. These pictures are very similar to those presented earlier in our paper describing the magnetic field measurements[5] and show local deposition under the focal spot as well as remote deposition out to the edge of the magnetized region.

As the overlayer thickness increases from 1—30 μm, the intensity of the central spot decreases while the intensity of the emission from the remote regions does not vary significantly until the overlayer becomes very thick (≥ 25 μm). This implies that the electrons penetrating the target beneath the focal spot have lower energy than those outside the focus. A similar result was obtained using 400-μm diameter targets irradiated at 2×10^{16} W/cm^2. In that case the integrated yield curve versus overlayer thickness (Fig. 1) deviated more significantly from the shape required for a Maxwellian distribution than was the case at the highest laser intensity. As a result, by integrating the emission from a number of penumbral pictures over regions of different diameter we obtained the curves shown in Fig. 5 which demonstrate graphically the relationship between electron energy and position on the target surface. If we now assume that the plasma acts as a

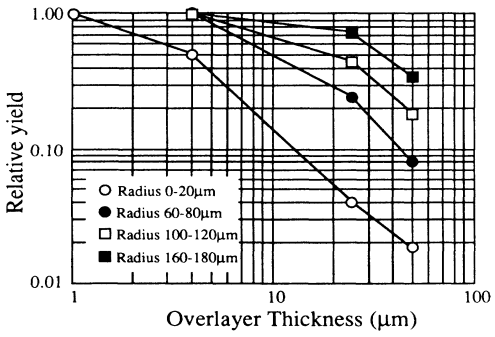

FIG. 5. The $K\alpha$ yield as a function of overlayer thickness spatially resolved over the target surface.

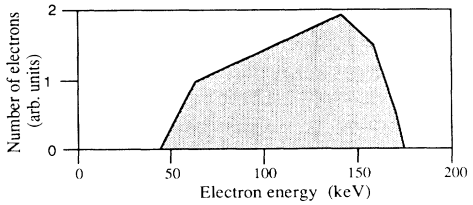

FIG. 6. The energy spectrum of the electrons entering the target deduced from the spatially resolved $K\alpha$ emission data.

sort of electron analyzer, returning different energy electrons to different regions of the target surface, we can use Fig. 5 to determine how the electron energy varied across the surface. We found that the electron energy increases monotonically with distance from the focus. This result is consistent with that reported by Keiffer *et al.*[19], but differs from the data presented in their earlier work.[24] It also contradicts the results of the computer simulation by Wallace,[4] although it is noted in that paper that there are a number of physical effects not included in the code that could reverse his conclusion that the most energetic electrons entered the target behind the laser-irradiated region.

The data shown in Fig. 5, together with absolute values for the $K\alpha$ yield as a function of electron energy and overlayer thickness calculated using the Monte Carlo code, can be converted into an electron energy distribution in the target which is shown in Fig. 6. This curve is far from being a Maxwellian. It quantitatively illustrates that the electron distribution was deficient in both high- and low-energy electrons.

IV. DISCUSSION

Our results provide the following picture of superthermal transport in disc targets irradiated using short-pulse, high-intensity, 1-μm laser radiation. Firstly, about 3% of the absorbed laser energy is deposited deep within the target by the superthermal electrons. As noted above, this is a value much lower than reported by other workers, although much of the discrepancy can be attributed to differences introduced through the use, in previous work, of the Spencer based model to predict the $K\alpha$ yield. It is worth noting that the $K\alpha$ yield depends strongly on the form of the electron distribution function and our work is the first where this has been measured.

Secondly, using a Monte Carlo electron-transport model to analyze the data on $K\alpha$ production in layered targets shows that a good fit to the space-integrated data could be obtained if the electron source was approximated by a monoenergetic beam entering the target. The beam energy increases with laser intensity according to the relationship $E_e \propto I^{(0.23\pm 0.05)}$.

Thirdly, the space-resolved data gave additional information which showed that the electron energy distribution in the target was rather more complicated than simply a monoenergetic beam. The energy of the electrons entering the target was found to vary over the surface with the lowest energy electrons appearing beneath the laser spot and the highest at the edge of the remote deposition region that extended up to about 200 μm from the focus.

The electron energy in fact increased monotonically with increasing radius as if the fields in the corona were acting as a sort of energy analyzer allowing the highest energy electrons to travel the furthest before returning to the target. This behavior is consistent with that reported by Fabbro and Mora[25] using their somewhat "rustic" model to map superthermal electron trajectories in a magnetized corona. They reported that the fastest electrons were those mainly responsible for the deposition remote from the focal spot. In contrast, Wallace[4] observed the opposite behavior in his simulations, namely, that the highest energy electrons entered the target behind the focus. Our evidence clearly contradicts Wallace's result.

The space-resolved data allowed the actual electron distribution to be determined which was shown in Fig. 6. The important feature of this distribution is that it is lacking in both low- and high-energy electrons. At the high-energy end, truncation of the spectrum can be expected when the superthermals are generated by collective mechanisms such as resonance absorption since the maximum electron energy will be limited by wavebreaking.[26] We considered the question of whether such a distribution was compatible with the wide range of data that exist on the superthermal x-ray spectrum which is almost universally interpreted by assuming that the superthermal electron energy distribution was Maxwellian. Most measurements of the superthermal x-ray spectrum have been made in the region below 100 keV (often below 50 keV) using a number (prehaps five or fewer) of K-edge filters combined with suitable x-ray detectors. The spectrum cannot be uniquely determined from such a small number of measurements but it is usually found that the data fit a Maxwellian distribution quite well. The electron distribution shown in Fig. 6 was found to generate a Bremsstrahlung spectrum which is very similar to that for a Maxwellian distribution in the region below 100 keV. In fact it is obvious that a K-edge filter spectrometer would not be able to distinguish between the two distributions. The resulting x-ray spectrum would be well fitted by a Maxwellian with a temperature of 60 keV which is in good agreement with previous measurements[27] of T_{hot}. Additionally, it is easy to show that if the x-ray spectrum produced by a monoenergetic beam were interpreted as due to a Maxwellian distribution with temperature T_{hot}, then $T_{\text{hot}} \approx E_e - E_x$, where E_e is the beam energy and E_x is the average photon energy at which the observations were made. As a result it is easy to see that T_{hot} drops more rapidly than E_e as the laser intensity decreases. Our results are, therefore, quite consistent with measurements of the intensity variation of T_{hot} which show a variable slope decreasing towards a value of 0.25 at high intensity in agreement with our value of 0.23 ($T_{\text{hot}} \propto E_e$ when $E_e \gg E_x$).

The electron energy distribution we have deduced is, in fact, quite similar to that reported by Terai *et al.*[28] from cannonball targets where modification of the coronal fields in their special target geometry was used to explain severe truncation at the high-energy end. Their results also showed a distinct lack of low-energy electrons entering the target as is the case here. We, therefore, require a mechanism which preferentially prevents the low-energy trons from entering the target (assuming that they are, in fact, generated[26]). One possibility is that the low-energy electrons may lose more of their energy in the corona in generating fast ions. This, at least qualitatively, fits the overall picture presented in the simulations.[1,25] In the absence of a detailed calculation of the energy spectrum of the electrons returning to the target surface, it is, however, difficult to prove. On the other hand, the electron energy distribution generated in the corona might well approximate a monoenergetic beam, as a simple mechanism involving wavebreaking of resonantly excited plasma waves would imply. In that case a reason why phase averaging does modify the distribution to form a quasi-Maxwellian distribution would be needed. If indeed, the mechanism generating the electrons produced a monoenergetic beam, this could be quite important in determining other interaction processes in the corona. The production of scattered "Raman" light via enhanced Thomson scattering is one example where the presence of such a beam would be important.[29]

There is an alternative explanation of our data which merit some discussion. The experimental data could be interpreted as indicating that the low-energy electrons apparently penetrate *further* than expected into the solid. It is possible, therefore, that our transport model is inaccurate because we have not included some phenomenon that actually *improves* low-energy electron transport. One possibility is that a magnetic field extends all the way through the solid behind the focus and prevents the electrons from being scattered radially across the magnetic field lines in this region, hence improving axial transport. This could result in the electrons traveling essentially straight through the target rather than along a random path as usually occurs. At first sight this seems rather unlikely, however, if the hot-electron current (which amounts to some 10 kA) were not locally neutralized as the electron beam traveled into the solid, this current is sufficient to establish a megagauss magnetic field which could collimate the electron beam, especially for medium- to high-energy electrons for which the collision frequency would be comparable with the electron cyclotron frequency. A brief investigation of the effect of a magnetic field on electron transport within the solid using the Monte Carlo code[30] demonstrated that transport could be enhanced for moderate energy electrons (≥ 50 keV). As yet, however, it is pure speculation that such fields exist. An experimental study to search for magnetic fields on the rear of the targets could, however, help clarify these ideas.

V. CONCLUSIONS

We have presented comprehensive experimental measurements of superthermal energy transport in laser-irradiated targets diagnosed using both time- and space-integrated $K\alpha$ emission from layered disc targets. The results have been analyzed with the aid of a Monte Carlo electron transport model in order to explain some unusual features. This has indicated that the electron distribution entering the target is non-Maxwellian. The spatially

resolved electron energy deposition patterns show that the electron energy, in fact, varies over the target surface. The results, when correlated with our previous measurements taken in similar conditions of self-generated magnetic fields, emphasize the important role the magnetic field plays in superthermal energy transport. Some of the more unusual features observed in these experiments can only be clarified by using complex computer models to study the details of the interaction within the corona and solid and such codes were not available to us in this study.

ACKNOWLEDGMENTS

The authors would like to thank Dr. M. Kalal for discussions of the effect of magnetic fields on transport within the solid, and Dr. R. Dragila for his critical comments.

*Present address: School of Physics, The University of Melbourne, Parkville, Victoria, Australia 3052.

[1]D. W. Forslund and J. U. Brackbill, Phys. Rev. Lett. **48**, 1614 (1982).
[2]P. A. Jaanimagi, N. A. Ebrahim, N. H. Burnett, and C. Joshi, Appl. Phys. Lett. **38**, 734 (1981).
[3]F. Amiranoff, E. Eidmann, R. Sigel, R. Fedosejevs, A. Maaswinkel, Yung-Lu Teng, J. D. Kilkenny, J. D. Hares, D. K. Bradley, B. J. MacGowan, and T. J. Goldsack, J. Phys. D **15**, 2463 (1982).
[4]Jon M. Wallace, Phys. Rev. Lett. **55**, 707 (1985).
[5]M. D. J. Burgess, B. Luther-Davies, and K. A. Nugent, Phys. Fluids **28**, 2286 (1985).
[6]J. D. Hares, J. Kilkenny, M. Key, and J. G. Lumney, Phys. Rev. Lett. **42**, 1216 (1979).
[7]M. D. J. Burgess, R. Dragila, B. Luther-Davies, K. A. Nugent, and G. J. Tallents, *Laser Interaction and Related Plasma Phenomena* (Plenum, New York, 1984), Vol. 6, p. 461.
[8]A. Perry, Ph.D. thesis, Australian National University, 1986.
[9]K. A. Nugent, and B. Luther-Davies, Opt. Commun. **49**, 393 (1984).
[10]N. H. Burnett, G. D. Enright, A. Avery, A. Loen, and J. C. Keiffer, Phys. Rev. A **29**, 2294 (1984).
[11]K. B. Mitchell, and R. P. Godwin, J. Appl. Phys. **49**, 3851 (1978).
[12]R. J. Harrach, and R. E. Kidder, Phys. Rev. A **23**, 887 (1981).
[13]L. V. Spencer, Phys. Rev. **98**, 1597 (1955).
[14]F. Salvat, and J. Parellada, J. Appl. Phys. **17**, 185 (1984); **17**, 1545 (1984).
[15]*Handbook of Spectroscopy,* edited by J. W. Robinson (Chemical Rubber Compancy, Cleveland, 1974), Vol. 1.
[16]H.-W. Drawin, Z. Phys. **164**, 513 (1961).
[17]E. Casnati, A. Tartari, and C. Baraldi, J. Phys. B **15**, 155 (1982).
[18]J. Jessenberger, and W. Hink, Z. Phys. **A275**, 331 (1975).
[19]J. C. Kieffer, H. Pépin, M. Piché, J. P. Matte, T. W. Johnson, P. Lavigne, and F. Martin, Phys. Rev. Lett. **50**, 1055 (1983).
[20]N. A. Dyson, *X-rays in Atomic and Nuclear Physics* (Longmans, London, 1973).
[21]G. D. Tsakiris, K. Eidmann, R. Petsch, and R. Sigel, Phys. Rev. Lett. **46**, 1202 (1981).
[22]R. L. Morse, Phys. Rev. Lett. **42**, 239 (1979).
[23]N. A. Ebrahim, C. Joshi, and H. A. Baldis, Phys. Rev. A **25**, 2440 (1982).
[24]R. Decoste, J. C. Kieffer, and H. Pépin, Phys. Rev. Lett. **47**, 35 (1981).
[25]R. Fabbro and P. Mora, Phys. Lett. **90A**, 48 (1982).
[26]B. Bezzerides, S. J. Gitomer, and D. W. Forslund, Phys. Rev. Lett. **44**, 651 (1980).
[27]D. W. Forslund, J. M. Kindel, and K. Lee, Phys. Rev. Lett. **39**, 284 (1977).
[28]K. Terai, H. Daido, M. Fujita, H. Nishimura, K. Mima, S. Nakai, and C. Yamanaka, Jpn. J. Appl. Phys. **23**, L445, (1984).
[29]A. Simon and R. W. Short, Phys. Rev. Lett. **67**, 153 (1984).
[30]M. Kalal (private communication).